Ordered mesoporous silica functionalized with β-cyclodextrin derivative for optical isomer separation of flavanones and flavanone glycosides by nano-liquid chromatography and capillary electrochromatography

Mariana Silva [a, b], Damián Pérez-Quintanilla [a], Sonia Morante-Zarcero [a], Isabel Sierra [a], María Luisa Marina [c], Zeineb Aturki [b], Salvatore Fanali [b]*

[a] *Departamento de Tecnología Química y Energética, Tecnología Química y Ambiental, Tecnología Mecánica y Química Analítica, E.S.C.E.T, Universidad Rey Juan Carlos, C/ Tulipán s/n, 28933 Móstoles, Madrid, Spain*

[b] *Institute of Chemical Methodologies, Italian National Council of Research, Area della Ricerca di Roma, Via Salaria Km 29, 300-00015 Monterotondo Scalo, Rome, Italy*

[c] *Departamento de Química Analítica, Química Física e Ingeniería Química, Facultad de Biología, Ciencias Ambientales y Química, Universidad de Alcalá, Ctra. Madrid-Barcelona Km 33.600, 28871 Alcalá de Henares, Madrid, Spain*

* Corresponding author. Tel.: + 39 0690672256; fax: + 39 0690672269.

E-mail address: salvatore.fanali@imc.cnr.it

ABSTRACT

In this paper a novel chiral stationary phase (CSP) was prepared by the immobilization of a β-CD derivative (3,5-dimethylphenylcarbamoylated β-CD) onto the surface of amino-functionalized spherical ordered mesoporous silica (denoted as SM) via a urea linkage using the Staudinger reaction. The CSP was packed into fused silica capillaries 100 μm I.D. and evaluated by means of nano-liquid chromatography (nano-LC) and capillary electrochromatography (CEC) using model compounds for the enantioseparation and the diastomeric separation. The compounds flavanone, 2′-hydroxyflavanone, 4′-hydroxyflavanone, 6-hydroxyflavanone, 4′-methoxyflavanone, 7-methoxyflavanone, hesperetin, hesperidin, naringenin, and naringin were studied using reversed and polar organic elution modes. Baseline optical isomers resolution and good results in terms of peak efficiency and short analysis time of all studied flavonoids and flavanones glycosides was achieved in reversed phase mode, using a mixture of MeOH/H_2O, 10 mM ammonium acetate pH 4.5 at different ratios as mobile phase. For the polar organic mode using 100 % of MeOH as mobile phase, the CSP showed better performances, the baseline chiral separation of several studied compounds occurred in an analysis time of less than 10 min. Also good results were achieved by CEC employing two different mobile phases. The use of MeOH/H_2O, 5 mM ammonium acetate buffer pH 6 (90/10, v/v) was very effective for the chiral resolution of flavanone and its methoxy and hydroxy derivatives.

Keywords: Nano-liquid chromatography; Capillary electrochromatography; Ordered mesoporous silica; Chiral separations; β-Cyclodextrin stationary phase; Flavanones

1. Introduction

The separation and analysis of chiral compounds is an important research topic in different fields also including analytical chemistry. A large number of compounds, possessing chiral centre (one or more), exist as one or more pairs of enantiomers. Two enantiomers may exert a different biological and/or pharmacological activity, especially when they are involved in biological processes also counting those related to human health. This is the case of drugs, pesticides, proteins, peptides, etc. For this given reason, the separation of chiral compounds is increasingly in demand in various application fields such as, pharmaceutical, agrochemical, biomedical, environment, nutraceutical areas [1]. Therefore, to meet the requirements related to the resolution and quantification of enantiomers, several stereoselective separation methods have been developed [2 - 7].

Analytical techniques so far used for enantiomers separation include gas chromatography (GC), supercritical fluid chromatography (SFC), thin-layer chromatography (TLC), high-performance liquid chromatography (HPLC) and capillary electrophoresis (CE) [2, 5 - 11]. In HPLC, the direct resolution method, employing chiral stationary phases (CSPs) is very popular. CSPs silica/titanium based or monolithic materials have been modified with various chiral selectors (CSs), i.e., cyclodextrins, polysaccharide derivatives, macrocyclic antibiotics, proteins, peptides, Pirkle-type, etc. [2, 5 – 8, 12 - 14]. In that respect, in the last years, thanks to recent achievements in the field of materials science, new chromatographic methods for enantiomers separation utilizing new CSPs have been developed [15]. In addition, the recent progress of miniaturized analytical techniques such as nano-/capillary liquid chromatography (nano-LC/CLC) or capillary electrochromatography (CEC) have

opened new horizons in the field of separation science. These techniques can be considered complementary or alternative to HPLC or CE. Column downscaling entails an important advantage over conventional HPLC columns, such as, limited sample and mobile phase volumes and the use of small amounts of expensive CSPs that decrease operating costs. Furthermore, these techniques offer good separation efficiency and resolution, shorter analysis time and rapid optimization of experimental conditions [3, 4, 16, 17]. New developments in the preparation of nanoparticles and monoliths as stationary phases for miniaturised liquid phase separation techniques have been reviewed recently [18].

Silica-based materials are very appealing for analytical applications because they are relatively inexpensive, thermally stable, chemically inert and biocompatible. The discovery of ordered mesoporous silicas (OMSs) in the early nineties marked the beginning of research in the development of high surface area materials with controlled porosity [19]. Other advantages of OMSs include i) better accessibility to binding sites due to open framework and regular structure, ii) high adsorption capacities, iii) better selectivity and faster adsorption rates. In addition, the dramatically higher surface area of OMs in comparison to commercially available chromatographic grade silica enhances resolution of molecules by increasing capacity factors to allow effective separations of analytes. Up to date, a variety of OMSs (MCM-41, SBA-15, HMS, MSU, etc.) have been proposed as stationary phases or supports to prepare stationary phases for solid phase extraction [20, 21] and chromatography [22].

Among the CSs used to develop CSPs, β-cyclodextrin (β-CD) and its derivatives have been extensively used for chiral separation employing different chromatographic modes. Cyclodextrins (CDs) are cyclic oligosaccharides formed by glucopyranose units linked by α(1,4) bonds. The common α-CD, β-CD and γ-CD are composed of 6, 7 and 8

glucose units, respectively. CDs are cone-shaped and present a hydrophobic environment in the interior of the cavity while the outer surface remains hydrophilic. These properties make them complex agents of first interest since they can include a great variety of molecules of appropriate polarity and size. CDs are widely used as CSs for the enantioresolution of drugs in separation techniques such as HPLC or CE [11, 23 - 31]. Although many CSPs based on CD are commercially available nowadays, there is a need to develop new packing materials offering high enantioselectivity in short analysis time. In this sense, the use of OMSs for CSPs preparation improves enantioselectivity and resolution with respect to the use of conventional silica grafted with the same chiral selector. The applicability of OMSs in chiral HPLC has been explored in some works [15]. However, to the best of our knowledge papers dealing with the use of CSPs based on OMSs for capillary/nano-LC have not been reported. On the other hand, only one paper has demonstrated the use of submicron MCM-41 modified with phenylcarbamoylated-β-CD as CSP in CEC, achieving rapid, base line resolution of racemic halogenated aryl alcohols and the β-blockers propanolol and pindolol, and higher enantioselectivity compared to capillaries packed with normal 3 and 5 μm silica [32].

In this work, a CSP by the immobilization of a β-CD derivative (3,5-dimethylphenylcarbamoylated β-CD) onto the surface of amino-functionalized spherical ordered mesoporous silica via a urea linkage using the Staudinger reaction [33] has been synthesized for the first time. The CSP showed good chiral resolution abilities toward optical isomers of flavanones and flavanone glycosides by nano-LC and CEC.

2. Experimental

2.1 Chemicals and samples

All chemicals were of analytical reagent grade and used as received. Tetraethylorthosilicate 98% (M = 208.33 g/mol, d = 0.934 Kg/m^3), poly(ethylene glycol)-block-poly(propylene glycol)-blockpolyethylene glycol, Pluronic 123 (M_{av} = 5800 g/mol, d = 1.019 Kg/m^3), cetyltrimethylammonium bromide (CTAB) 98%, (M = 364.46 g/mol), β-CD, ethyl acetate, pyridine, 3,5-dimethylphenyl isocyanate 99 %, sodium azide and 3-aminopropyltriethoxysilane were purchased from Sigma-Aldrich (St. Louis, USA). Hydrochloric acid 37%, acetone, ethyl ether, ethanol and anhydrous sodium sulphate were purchased from Scharlau (Barcelona, Spain). Acetonitrile (AcN), methanol (MeOH), ethanol (EtOH), isopropanol (i-PrOH), acetone and n-hexane (n-Hex) were purchased from Carlo Erba (Milan, Italy). A Milli-Q system (Millipore Waters, Milford, MA, USA) was employed to deionize the water. Ammonium acetate (500 mM), utilized for the chromatographic runs, was obtained by titrating the appropriate volume of acetic acid with concentrated ammonia solution to pH 4.5. Mobile phases employed for the nano-LC experiments were daily prepared by mixing suitable volumes of buffer solution, water and organic solvents (AcN or MeOH). LiChrospher 100 RP-C_{18}, 5 μm particle diameter, was from Merck (Darmstadt, Germany). Fused silica capillaries, 100 μm I.D. x 360 μm O.D. were purchased from Polymicro Technologies (Phoenix, AZ, USA). The selected flavonoids (flavanone, 2′-hydroxyflavanone, 4′-hydroxyflavanone, 6-hydroxyflavanone, 4′-methoxyflavanone, 7-methoxyflavanone, hesperetin, hesperidin, naringenin, and naringin) were from Sigma–Aldrich (St. Louis, MO, USA). Stock standard solutions of each flavonoid (1 mg/mL)

were prepared in MeOH, and stored at 4ºC. Further dilutions were daily done with water and AcN (60:40, v/v) to obtain the final concentration of 100 μg/mL.

Fig 1S. shows the chemical structure of the studied compounds (supplementary material).

2.2 Instrumentation

A BASIC 20 pH meter (Crison, Barcelona, Spain) was employed for accurate pH measurements in aqueous buffer solution. A Series 10 LC HPLC pump (Perkin Elmer, Palo Alto, CA, USA) a Decon model FS 100b (Hove, UK) ultrasonic bath and a Stereozoom 4 optical microscope (Cambridge Instruments, Vienna, Austria) were employed for the capillary packing process.

The nano-LC experiments were carried out with a laboratory-assembled instrumentation utilizing a LC10 HPLC pump (Perkin Elmer, Palo Alto, CA, USA), a modified injection valve (Enantiosep GmbH, Münster, Germany), and an UV–vis on-column detector (Spectra Focus PC1000, Thermo Separation Products, San Jose, CA, USA), set at 200 nm. The HPLC pump, delivering continuously MeOH isocratically, and the injector were connected so as to obtain a passive split-flow system needed to reduce the flow rate at nL/min levels. The capillary column was directly inserted into the modified injector equipped with 50 μL loop. Both pump and injection valve were joined to a stainless steel T piece (Vici, Valco, Houston, TX, USA) by means of 500 μm I.D. stainless steel tubes with lengths of 70 and 5 cm, respectively. The third entrance of the T was connected to the MeOH reservoir of the pump, through a fused silica capillary (50 μm I.D. × 20 cm) achieving a continuous recycling of the organic solvent.

Sample and mobile phase were introduced into the nano- LC system through the injection valve. Injections were done by filling the loop with the sample solutions, switching the valve for appropriate time and then flushing the loop with the mobile phase.

The flow rate was estimated by connecting a 10 μL syringe (Hamilton, Reno, NV, USA) to the capillary column outlet through a Teflon tube (TF-350; LC-Packing, CA, USA) and by measuring the volume of mobile phase accumulated over 5 min.

Data were collected using Clarity™ Advanced Chromatography Software (DataApex Ltd., Prague, Czech Republic).

CEC experiments were performed on a HP^{3D} CE apparatus (Agilent Technologies, Waldbronn, Germany) with on-column UV-diode array detector operating at 214 nm. The same capillary column employed in nano-LC containing the packed CSP with different length of 23 cm (total length, 33.5 cm) was used for the enantiomers separation. During runs the two electrode compartments were pressurized at 10 bar to avoid bubble formation. A voltage of -15 kV was applied during CEC experiments. Samples were injected by hydrodynamic method (8 bar x 0.5 min). Data were recorded with Chemstation software (Rev. A.09.01, Agilent Technologies)

2.3 Preparation of stationary phases

A new β-CD-derived CSP was prepared through the Staudinger reaction [33] between aminopropyl silica and a carbamoylated β-CD derivative. Fig. 1 shows the synthesis procedure of the CSP, starting from the preparation of 3,5-dimethylphenylcarbamoylated β-CD and amino-functionalized spherical ordered mesoporous silica (SM-NH_2).

2.3.1 Preparation of 3,5-dimethylphenylcarbamoylated β-CD

Firstly, monotosyl-β-CD (compound **1**) was prepared taken as reference the method of Pasqua et al. [34], with some modifications. Dried β-CD (13.0 g) was added in portions with stirring to a 500 mL round bottom flask containing 100 mL of anhydrous pyridine until complete dissolution was achieved. Tosyl chloride (1.7 g) was then added in portions over a period of 40 min with stirring. The resulting clear solution was allowed to stand at room temperature for 18 h. Pyridine was then removed in vacuum, and the residual oil was triturated with acetone. The resulting solid was filtered and washed with acetone. After this, the solid was transferred into a 500 mL flask together with 150 mL of water and stirring overnight at room temperature. The resulting precipitated was filtered, washed with water and dried under high vacuum for 12 h. Then, in order to obtain the azido β-CD (compound **2**), dried compound **1** (1.0 mmol) and an excess of sodium azide (5.0 mmol) were dissolved in 200 mL of water and heated for 18 h at 86 °C (see Fig. 1). The solvent was reduced to ca. 50 mL with distillation in vacuum. For purification by complex formation, tetrachloroethane (15 mL) was added and the mixture was stirred for 15 min at room temperature. The complex formed was separated from the aqueous solution by centrifugation, heated at 100 °C (30 min) and dried under high vacuum for 4 hours [35]. Characterization data for compound **2**: FT-IR (cm^{-1}, ATR): 3302 (O-H str), 2924.5 (C-H str), 2108.7 (N_3 str), 1020.7 (C-O str)

Finally, 1 mmol of dried compound **2** was dissolved in 20 mL of anhydrous pyridine and 25 mmol of 3, 5-dimethyl phenyl isocyanate was added and allowed to stir overnight at room temperature. The pyridine was removed by vacuumed distillation. The solid was dissolved in 100 mL of ethyl acetate and filtered to eliminate rest of

unsolved solid. The mixture was washed three times with 100 mL of brine (10% , p/v) and the solid dried in anhydrous sodium sulphate. The ethyl acetate solution was concentrated to about 25 mL and 100 mL of hexane was added to the concentrated, the suspension was filtrated to eliminate rest of solid. Finally the ethyl acetate was evaporated and the obtained solid (3,5-dimethylphenylcarbamoylated β-CD, compound **3**) was dried for 8 hours at 65 °C. Characterization data for compound **3**: FT-IR (cm^{-1}, ATR): 3393-3309 (amide N-H str), 3015 (arom C-H str), 2919 (C-H str), 2108.7 (N3 str), 1714 (ester C=O), 1613, 1538, 1437 (arom C=C), 1212, 1042 (C-O-C). ^{1}H NMR ($CDCl_3$, TMS) δ (ppm) 6.92-6.42 (m, C_6H_3); 5.96-5.55, 5.16-4.67, 4.12-3.94 (m, β-CD); 2.04-1.26 (m, CH_3).

2.3.2 Preparation of amino-functionalized spherical ordered mesoporous silica

Spherical mesoporous silica (denoted SM) was prepared according to our previous work [36]. Typically, 18 g of Pluronic 123 and 3 g of CTAB were dissolved in a solution formed by mixing 360 mL of 2 M HCl, 180 mL H_2O and 150 mL ethanol. Then, 60 mL of TEOS were added in the aqueous solution at room temperature under magnetic stirring. After 30 min of stirring, the solution was transferred into a Teflon-lined steel Parr autoclave and heated at 80℃ for 5 h, and then kept at a higher temperature (130 ℃) for 12 h. The white precipitate was filtered off and washed with Milli- Q water, dried at 90℃ for 24 h, and calcined in air at 550℃ for 5 h to remove the template.

SM (5.2 g heated at 150 °C for 20 h) was suspended in 40 mL of toluene and 2.6 mL of 3-aminopropyltriethoxysilane were added (1/2, m/v), in order to obtain amino

functionalized SM (SM-NH_2). The mixture was heated at 8 °C for 24 h at 500 rpm. The solid was washed with two fractions of 50 mL of toluene, ethanol and ethyl ether.

2.3.3 Funcionalization of SM-NH_2 with 3,5-dimethylphenylcarbamoylated β-CD

Derivatization of SM-NH_2 with compound **3** was carried out according to the Staudinger reaction under mild reaction conditions [33]. 2.3 g of SM-NH_2 were stirred in 25 mL of anhydrous THF under a CO_2 atmosphere (flow 2 bar). After 10 min, a solution of compound **3** in 20 mL of anhydrous THF was added and stirring with CO_2 bubbled for 5 min. Then was added 1 g of triphenylphosphine in 20 mL of THF. The mixture was stirred with constant bubbling of CO_2 for 21 h. Followed the solid was washed with 100 mL of THF and then with Soxhlet extraction with acetone for 48 h to remove the triphenylphosphine oxide and any unreacted cyclodextrin by-products. Finally the solid (denoted as SM-β-CD) was dried for 72 h at 60 °C.

2.4 Characterization of the mesoporous silicas

X-ray diffraction (XRD) patterns of mesoporous silicas were obtained on a Philips diffractometer model PW3040/00 X´Pert MPD/MRD at 45kV and 40mA, using Cu Kα radiation (λ= 1.5418 Å). Scanning electron micrographs and morphological analysis were carried out on a XL30 ESEM Philips with an energy dispersive spectrometry system. Conventional transmission electron microscopy was carried out on a TECNAI 20 Philips, operating at 200 kV. Proton-decoupled ^{29}Si and ^{13}C MAS NMR spectra were recorded on a Varian-Infinity Plus Spectrometer at 400 MHz. N_2 gas adsorption–desorption isotherms were obtained using a Micromeritics ASAP 2020

analyzer, and pore size distributions were calculated using the Barrett–Joyner–Halenda (BJH) model on the desorption branch. Elemental analysis (% C, % N, % H) was performed with a LECO CHNS-932 analyzer (Universidad Rey Juan Carlos, Spain). The thermal stability of the modified mesoporous silicas was studied using a Setsys 18A (Setaram) thermogravimetric analyzer (from 25 to 800 ºC at 10 ºC/min).

2.5 Preparation of capillary columns

The capillary columns (100 μm I.D. x 375 μm O.D. x 50 cm) were packed following a previous reported procedure [2, 37]. Briefly, one end of the capillary was connected to a mechanical temporary frit, Valco (Houston, TX, USA) to retain the packing material and the other end to a stainless steel HPLC pre-column (50 mm × 4.1 mm I.D.), which was used as reservoir of the slurry. A series LC10 pump, PerkinElmer (Palo Alto, CA, USA) was used for the packing procedure.

The capillary was firstly packed to 10 cm with LiChrospher 100 RP-C_{18} stationary phase suspended in MeOH (3-5 mg in 1 mL) for the frit preparation. Then the slurry was removed from the pre-column and the capillary flushed with water (about 15 min). The frit was prepared by sintering the RP-C_{18} for 8 s at about 700 ºC with a heated wire (laboratory made apparatus). This was done flushing continuously with water. After removing the temporary frit, the capillary was flushed with MeOH followed by i-PrOH to eliminate the excess of packing material. Afterwards the column was packed with the CSP suspended in i-PrOH to 20 cm. Finally, the column was packed again with the RP-C_{18} particles to prepare the second frit following the same procedure applied for the first one. The detection window was prepared at 2 cm to the outlet frit by removing the outside polyimide layer with a razor.

2.6 Calculation of chromatographic parameters

The resolution factor, *Rs*, was calculated according to the following formula:

$$Rs = 2\frac{tr2-tr1}{W1+W2} \qquad (1)$$

where t_{r1} and t_{r2} are the retention times of the enantiomers and w_1 and w_2 are the peak widths at baseline.

3. Results and discussion

3.1 Synthesis and characterization of the mesoporous silicas

By virtue of the interesting applications of CD-based CSP in different separation techniques, numerous publications about novel synthethic routes and/or immobilization strategies have emerged during the last years [38]. However, in some of these preparation methods, regioselective immobilization of β-CD cannot be readily accomplished, since the hydroxyl groups at 2, 3 and 6 position of β-CD could react with the functional group on the solid support and multi-linked β-CDs CSP would be formed (instead of one with well-defined chemical structure). In addition, subsequent chemical derivatization of the immobilized β-CD (using a heterogeneous synthetic route), usually leads materials with low batch-to-batch reproducibility. To overcome these problems, in this paper SM was functionalized using a homogeneous synthetic route. For this purpose, mono(6-azido-6-deoxy)perfunctionalized β-CD was first synthesized and purified, and then this derivative was immobilized onto the surface of amino-functionalized SM (SM-NH_2) using the Staudinger reaction [33]. In these conditions,

the chemical anchoring of the β-CD derivative onto the mesoporous silica support was effective via the hydrolytically stable urethane linkage (Fig. 1). Since only purified compound **3** was used and only one active azido-functional group was presented in every molecule of this compound, where the reaction takes place, the current procedure afforded a structurally well-defined β-CD based CSP.

The XRD patterns of the obtained SM material (Fig. 2A) exhibit a single (100) diffraction peak at low angle region (0.93º). In this material the d_{100} spacing, assigned to the pore-to-pore centre correlation distance, was 94.9 Å. This pattern is typical of materials with uniform pores in the mesoporous range and non-symmetrical 3-D wormhole-like structure of the porous framework, with a pore structure lacking long-range order. XRD pattern of the modified SM-β-CD (Fig. 2B) indicates that the basic pore structure of the material remains unchanged after functionalization, an the decrease in XRD signal intensity can be attributed to the presence of the β-CD groups inside the pore channels of the material [39]. In addition, the increase in the wall thickness, from 15.04 Å in SM to 57 Å in SM-β-CD, confirmed that the functionalization occurred also inside the mesopore channels.

Fig. 2C shows N_2 adsorption-desorption isotherms for SM, SM-NH_2 and SM-β-CD materials. All the isotherms are type IV according to the IUPAC classification with hysteresis loops type H1, which are representative of mesoporous materials. At low relative pressures P/P_0, between 0 and 0.3 the nitrogen adsorption is produced in monolayer. At pressure upper 0.3 capillarity condensation and pores filling occur. The isotherms of the modified materials (SM-NH_2 and SM-β-CD) were of the same type than the non-modified material (SM), with a reduction in the adsorbed volume and in the hysteresis loop due to the decrease in the pore size that takes place when the ligand is attached into the pores. These results showed an important decrease in the surface

area (from 660.66 to 389.36 m^2/g), pore diameter (from 74.5 to 45.6 Å) and pore volume (1.2 to 0.54 cm^3/g) after the functionalization with the β-CD derivative (see Table 1S in supplementary information). Thus, it can be inferred that the β-CD groups were grafted not only to the external surface area of the mesoporous silica particles, but also inside the mesostructured pore channels. This fact agrees with the results obtained by other authors who indicated that only with pore diameters > 60 Å the β-CD moieties can react with the anchoring sites ($-NH_2$) inside the pore channels [39]. Fig. 2D shows the pore size distribution of the materials after and before the functionalization procedure.

NMR spectroscopy is one of the most powerful techniques for verifying the incorporation of functional groups by enabling the simultaneous identification of multiple functionalities, as well as, the different types of silanol groups and the effectiveness of the covalent bonding of the ligand to the silica framework. The ^{29}Si MAS NMR and ^{13}C MAS NMR spectra of these new materials corroborate the presence of the β-CD derivative groups. ^{29}Si MAS NMR spectra of SM and SM-β-CD are showed in Fig. 3A and 3B. In these spectra, resonances around -110 ppm, -105 ppm and -92 ppm can be assigned as Q^4 [$(SiO)_4$***Si***], Q^3 [$(SiO)_3$***Si***-(OH)] and Q^2 [$(SiO)_2$***Si***-$(OH)_2$] sites, respectively. Clearly, Q^4 is the dominant peak because it is the most abundant site. In addition, the two other peaks that appeared at -55 and -65 ppm in the SM-β-CD spectrum (Fig. 3B) were assigned to T^2 ($(SiO)_2$***Si***OH-R) and T^3 ($(SiO)_3$***Si***-R) sites, respectively, and corroborated the covalent attachment of the organic ligand in this material. The ^{13}C CP-MAS NMR spectrum of SM-β-CD (see Fig. 2S in supplementary material) shows peaks in the central spectral region (ca. δ = 98.8 - 58.3 ppm) typical of cyclodextrin units. The peaks for the triehoxysilane unit (**C**H_2**C**H_2**C**H_2Si) are observed at ca. δ = 10 – 42 ppm and the urethane linkage (O**C**ONH) was observed at ca. δ = 160

ppm. Finally, signals observed at ca. δ = 110 -140 ppm are assigned to the carbon atoms of phenylcarbamoyl groups. Results of NMR spectroscopy are in agreement with other works [34, 40, 41] and confirmed the presence of β-CD derivative into the SM structure and, therefore, the right functionalization of the material.

The morphology, shape and size of the particles of the prepared materials were studied by SEM. SEM micrographs showed that materials had a spherical morphology (Fig. 4A), with a very good particle circularity factor centered at 0.87 (Fig. 4B). In addition, a reasonable distribution of particle size (dispersity) to have good column packing quality was achieved, with the vast majority of the particles in the range of 4 – 6 μm. This particle size distribution is in agreement with previous synthesis of mesoporous materials type SM [36]. SEM images for the SM-β-CD material show that the morphology and size of the particle remains similar after the funtionalization process. Fig. 4B shows a SEM image of cutting section of 100 μm I.D. capillary column, where the column bed formed by the spherical SM-β-CD particles can be observed. On the other hand, TEM images of these silicas show irregularly aligned mesopores throughout the materials with relatively uniform pore sizes (wormhole-like pore arrangement). These results are in good agreement with the related XRD patterns and N_2 adsorption–desorption isotherms.

The amount of aminopropyl groups and β-CD derivative attached onto the silica surface was calculated by the % N and % C obtained by elemental analysis in both SM-NH_2 and SM-β-CD materials. Results obtained indicated that the SM-NH_2 material had a functionalization degree of 1.38 mmol/g. After the immobilization of the β-CD derivative (compound **3**) onto its surface, via the Staudinger reaction, the residual aminopropyl groups were estimated in 1.27 mmol/g. These results confirmed that due to steric hindrance it was not possible to functionalize all the amino groups of the material.

On the other hand, functionalization degree of the SM-β-CD was 32 μmol/g with a CD surface coverage of 8.22 x 10^{-8} mol/m^2. TGA curves of the prepared silicas (see Fig. 3S in supplementary material) showed that exothermic degradation processes occur in the range of 200 – 600ºC, with weight loss of 7 and 20% in SM-NH_2 and SM-β-CD, respectively, that demonstrated good thermal stability of these modified materials. These characterization results confirmed that the SM-β-CD material was successfully prepared as a new type of CSP.

3.2 Chromatographic evaluation

In this work CSPs were packed into fused silica capillaries and the enantioresolution capability was evaluated by means of nano-LC for chiral separation of several flavanones (Fig. 1S in supplementary material).

The novel CSP studied contained a modified □-cyclodextrin. Therefore, the enantioresolution mechanism expected is an inclusion-complexation one. However, other additional mechanisms based on adsorption have also to be considered. Therefore, the composition of mobile phase must be carefully controlled to achieve optimal enantiomers separation. For this purpose, the enantioselectivity was evaluated under reserved and polar-organic elution modes. Mobile phases containing AcN and/or MeOH, with or without water buffered with ammonium acetate.

3.2 Evaluation of the chiral stationary phase using reversed-phase conditions

3.2.1 Influence of acetonitrile content in the mobile phase on nano-LC separation

Based on our experience and on data reported in literature, racemic model mixtures of compounds of nutraceutical interest have been chosen. Their enantiomeric separation was studied by nano-LC using the novel SM-β-CD CSP. The following flavonoids were studied: flavanone, 2′-hydroxyflavanone, 4′-hydroxyflavanone, 6-hydroxyflavanone, 4′-methoxyflavanone, 7-methoxyflavanone, hesperetin, hesperidin, naringenin, and naringin. Preliminary experiments were carried out using the reversed phase elution mode. Mixtures of AcN/H_2O, 10 mM ammonium acetate pH 4.5 at different ratio (40 - 90 % of AcN, v/v) were used as mobile phase. Flow rates in the range 225-281 nL/min were applied.

The plot of Ln *k* vs AcN concentration of the first eluted enantiomer (when resolved) showed a linear behaviour for all studied compounds. Therefore, from these experiments, it can be deduced that the chromatographic mechanism is of reversed-phase type. Fig. 5 gives an idea about the linear relationship observed. As can be seen, the increase of the organic solvent concentration in the mobile phase caused a reduction of retention factor (*k*) for the representative compounds 7-methoxyflavanone and flavanone. This was mainly due to the competition enantiomers/AcN with the hydrophobic CD cavity. The organic solvent had higher affinity [42]. Similar trend was observed for all other compounds.

Retention times (t_r) and enantioresolution factors (R_s) also decreased by increasing the AcN concentration for all analyzed compounds. For example, eluting with AcN/H_2O, 10 mM ammonium acetate pH 4.5 (40:60, v/v), t_r and R_s of 7-methoxyflavanone (first eluted enantiomer) were 33.0 min and 2.0, respectively. The two parameters decreased to 4.4 min and Rs = 0 increasing the content of organic

solvent at to 90 %. Flavanone baseline resolved in its enantiomers was achieved using AcN/H_2O, 10 mM ammonium acetate pH 4.5 (40:60, v/v) (*Rs* = 1.80, t_r = 38.4 min). On the other hand, the enantioresolution was completely lost and the t_r was reduced to 4.3 min employing 90 % of AcN.

Table 1 reports the chromatographic parameters, t_r, k, selectivity (α) and R_s under optimal experimental conditions. As can be seen, good resolution was achieved for flavanone and 7-methoxyflavanone, for the other compounds poor enantioresolution was obtained with R_s values in the range 0.00 - 0.8. These values are possible because the position of the substituent groups in the structure of the other flavanones is not favourable and the interaction with the CSP is not enough to show good R_s. In addition, AcN could hidden the formation of stereoselective interaction between the stereogenic centre and the functional groups of the CSP.

Fig. 6 shows the chromatograms of some flavanones enantiomers resolved under reversed-phase conditions by using a mixture of AcN/H_2O, 10 mM ammonium acetate pH 4.5 (40:60, v/v) as mobile phase.

3.2.2 Influence of methanol content in the mobile phase on nano-LC enantioseparation

Further experiments were carried out using the same capillary column and a mobile phase containing a different organic solvent. MeOH was selected instead of AcN and used at concentration range of 70 - 95 % (v/v). The organic solvent was mixed with 10 mM ammonium acetate buffer at pH 4.5. Lower concentrations of MeOH were not studied because by working in this range the separation of all compounds was obtained. In addition, at lower MeOH concentration, the t_r began to be high without increasing the resolution of compounds.

The increase of MeOH in the mobile phase caused a decrease of *k*. The plot of Ln *k* vs organic solvent concentration was linear for all studied compounds confirming, also with this solvent, a typical reversed phase mechanism at least at the concentrations studied.

The use of MeOH instead of AcN gave better results for analysis times and enantioresolution. For example, at 95 % MeOH concentration all analyzed compounds were resolved in their enantiomers or diastereoisomers with the exception of naringin.

Table 2 summarizes the chromatographic data, t_r, *k*, α and R_s of all flavanones tested at the optimized separation conditions. As can be seen, the highest R_s values were achieved for flavanone and for all methoxyflavanones. Lower R_s values were achieved for 2´-hydroxyflavanone, naringin, naringenin and hesperidin. Hesperetin showed a higher R_s value relative to its correspondent glycosidic compound hesperidin. These results could be explained by the fact that hesperetin exhibited a higher degree of interaction due to the higher hydrophobicity and smaller size of the aglycone molecule, allowing a greater affinity for the CD cavity [3]. In the same form more or less with naringenin and naringin. Fig. 7 shows the nano-LC separation of the studied enantiomers or diastereoisomers achieved at the optimal experimental conditions. As can be seen, peaks obtained show very good symmetry. This fact can be due to the high surface area and ordered pore structure of the mesoporous silica, which offers quick mass transfer kinetics during separation.

The better results with MeOH than AcN was due to the weaker displacing effect of MeOH that allowed a greater inclusion complex formation between the analyte and the CD cavity [43]. In addition, MeOH have an amphiprotic nature and the polar interactions gave a contribution to the chiral recognition [44]. Experiments performed

using EtOH or i-PrOH instead of MeOH revealed not satisfactory results concerning enantioresolution.

3.2.3 Influence of the buffer added to the mobile phase on nano-LC separation

The influence of buffer addition to the mobile phase on retention and enantioresolution was also studied. The presence of a buffer system can produce a variation in peak efficiency, enantioresolution and analysis time. The buffer composition can modify the hydrophobic nature of the analytes varying the non-covalent interactions between analytes and the CD cavity [4]. But, the flavanones investigated, except hesperetin and naringenin, are neutral and the CSP consequently is expected to have a little or no influence on the enantioseparation. Ammonium acetate buffer in the range 0 - 20 mM was investigated, keeping constant the organic modifier content. When buffer concentration was increased, no significant effect on enantioresolution was observed. The addition of a buffer system to the mobile phase did not affect the enantioresolution of flavanones significantly.

3.3 Evaluation of the chiral stationary phase using organic polar-phase conditions

The SM-β-CD CSP was finally studied in polar organic mode by using 100% AcN or MeOH as mobile phase, without any additives. With 100% AcN as mobile phase, no enantioseparation was achieved for all the studied compounds. Since the C-H bonds of AcN have a very high pKa value, the solvent will be aprotic [45]. But with MeOH 100%, all analysed compounds were resolved in their enantiomers or

diastereoisomers with the exception of naringin, naringenine and hesperidine. Fig. 8 and Table 3 shows these results.

4. Capillary electrochromatography

The novel capillary CSP column was also studied analyzing the same model standard racemic mixtures used in nano-LC with CEC. As reported in literature, the driving force of analytes and mobile phase into the column is the electroosmotic flow (EOF) generated by the application of a relatively high electric field. The EOF can move in the direction of either cathode or anode depending on some experimental conditions such as, the charge of the stationary phase, the composition of the mobile phase, the applied electric field, etc. Therefore, these parameters must be carefully selected and controlled. First of all, we selected a reversed polarity mode (EOF to anodic direction) just considering the chemical structure of the CSP (see Fig. 1) where positively charged amino groups close to the CDs are present. Just to compare CEC data with the ones achieved by nano-LC, the same mobile phase was tested. MeOH and/or AcN with water also containing ammonium acetate were selected. The presence of the buffer was necessary in order to have sufficient electric conductivity during the runs.

Table 4 shows the CEC data achieved analyzing flavanone and its derivative enantiomers employing two different mobile phases. The use of MeOH/H_2O, 5 mM ammonium acetate buffer pH 6 (90/10, v/v) was very effective for the chiral resolution of flavanone and its methoxy and hydroxy derivatives. R_s in the range 1.34 - 6.24 were obtained, while relatively long retention times were achieved (16.9 - 25.5 min, second eluted enantiomer).

The composition of the mobile phase was modified keeping constant the content of MeOH and the ionic strength, decreasing water concentration to 5% and adding 5% of AcN. As can be observed in Table 4 retention times decreased due to both increase of EOF and decrease of interactions with the CSP. This is documented by the decrease of retention factors. In addition, resolution factors decreased with poor enantioresolution of 2'-hydroxyflavanone. No peaks were detected for hesperetin, hesperedin, naringin and naringenin. As an example of the good performace of CEC, Fig. 9 shows some representative electrochromatograms achieved using the two mobile phases with and without AcN in the mixtures. As indicated previously, ordered mesoporous silicas possess a larger surface/volume ratio than conventional silica gel, which is important in chromatography for achieving favourable mass transfer. In that respect, considering the high surface area and special pore structure of ordered mesoporous silicas, symmetric peaks with little peak broadnening could be achieved with the new CSP developed.

4. Conclusions

A novel chiral stationary phase (CSP) has been successfully prepared and characterized, using spherical ordered mesoporous silica (SM) as support. Amino-functionalized SM was modified with 3,5-dimethylphenylcarbamoylated β-CD (SM-β-CD) and its potential of application as CSP, in nano-liquid chromatography (nano-LC) and capillary electrochromatography (CEC), was evaluated for the first time. Flavanones and flavanone glycosides were used as model compounds for the enantioseparation and the diastomeric separation. The analyses were carried out in capillary columns of 100 μm I.D. packed with the SM-β-CD. In nano-LC, the chiral separation of all studied compounds was obtained in reversed phase mode using a mixture of MeOH/H_2O, 10

mM ammonium acetate pH 4.5, at different ratios, as mobile phase. Although good results were achieved, polar organic phases (100% AcN or MeOH) were not as effective as the reverse phase conditions for the separation of these compounds. On the other hand, in CEC, the use of MeOH/H_2O, 5 mM ammonium acetate buffer pH 6 (90/10, v/v) was very effective for the chiral resolution of flavanone and its methoxy and hydroxy derivatives.

The use of the novel CSP in the nano-LC system allowed achieving the separation of enantiomers and diastereoisomers of flavanones with good results. Comparing the data about chiral resolution of these compounds with CSPs based on commercial silica gel derivatized with different β-CD derivatives in HPLC [43, 45] and nano-LC [3], it can be concluded that, in general, higher enantioresolution and shorter analysis time can be obtained with the CSP prepared and evaluated in this paper. Moreover, be due to the high surface area and ordered pore structure of the OMSs, symmetric peaks with little peak broadening could be achieved with the new CSP developed. In summary, these studies demonstrated that OMSs possess a promising potential as supports to develop new CSPs for nano-LC and CEC applications.

Acknowledgment

Authors thank the Ministry of Economy and Competitiveness (Spain) for research project CTQ2013-48740-P and the Comunidad of Madrid and European funding from FEDER program (project S2013/ABI-3028, AVANSECAL).

Appendix A. Supplementary data

Supplementary data associated with this article can be found, in the online version

References

[1] N. M. Maier, P. Franco, W. Lindner, Separation of enantiomers: needs, challenges, perspectives, J. Chromatogr. A 906 (2001) 3-33.

[2] A. Cavazzini, G. Nadalini, F. Dondi, F. Gasparrini, A. Ciogli, C. Villani, Study of mechanisms of chiral discrimination of amino acids and their derivatives on a teicoplanin-based chiral stationary phase, J. Chromatogr. A 1031 (2004) 143-158.

[3] K. Si-Ahmed, F. Tazerouti, A. Y. Badjah-Hadj-Ahmed, Z. Aturki, G. D´Orazio, A. Rocco, S. Fanali, Optical isomer separation of flavanones and flavanone glycosides by nano-liquid chromatography using a phenyl-carbamate-propyl-β-cyclodextrin chiral stationary phase, J. Chromatogr. A 1217 (2010) 1175-1182.

[4] K. Si-Ahmed, F. Tazerouti, A. Y. Badjah-Hadj-Ahmed, Z. Aturki, G. D´Orazio, A. Rocco, S. Fanali, Analysis of hesperetin enantiomers in human urine after ingestion of bloodorange juice by using nano-liquid chromatography, J. Pharmaceutical and Biomedical Analysis 51 (2010) 225–229.

[5] C. L. Barhate, Z. S. Breitbach, E. C. Pinto, E. L. Regalado, C. J. Welch, D. W. Armstrong, Ultrafast separation of fluorinated and desfluorinated pharmaceuticals using highly efficient and selective chiral selectors bonded to superficially porous particles, J. Chromatogr. A 1426 (2015) 241–247.

[6] C. L. Barhate, M. F. Waha, Z. S. Breitbach, D. S. Bell, D. W. Armstrong, High efficiency, narrow particle size distribution, sub-2 μm based macrocyclic glycopeptide chiral stationary phases in HPLC and SFC, Anal. Chim. Acta 898 (2015) 128–137.

[7] D. Albals, Y. V. Heyden, M. G. Schmid, B. Chankvetadze, D. Mangelings, Chiral separations of cathinone and amphetamine-derivatives: Comparative study between

capillary electrochromatography, supercritical fluid chromatography and three liquid chromatographic modes, J. Pharm Biomed. Anal. 121 (2016) 232-243.

[8] M. F. Wahab, R. M. Wimalasinghe, Y. Wang, C. L. Barhate, D. C. Patel, D. W. Armstrong, Salient Sub-Second Separations, Anal. Chem. 88 (2016) 8821−8826.

[9] G. K. E. Scriba, Chiral Recognition in Separation Science–An Update, J. Chromatogr. A 1467 (2016) 56-78.

[10] D. C. Patel, M. F. Wahab, D.W. Armstrong, Z. S. Breitbach, Advances in high-throughput and high-efficiency chiral liquid chromatographic separations, J. Chromatogr. A 1467 (2016) 2-18.

[11] J.M. Saz, M.L. Marina, Recent advances on the use of cyclodextrins in the chiral analysis of drugs by capillary electrophoresis, J. Chromatogr. A 1467 (2016) 74-94.

[12] O. H. Ismail , L. Pasti , A. Ciogli , C. Villani , J. Kocergin, S. Anderson, F. Gasparrini , A. Cavazzini , M. Catani, Pirkle-type chiral stationary phase on core–shell and fully porous particles: Are superficially porous particles always the better choice toward ultrafast high-performance enantioseparations?, J. Chromatogr. A 1466 (2016) 96-104

[13] N. Grecsó, E. Forró , F. Fülöp, A. Péter, I. Ilisz, W. Lindner, Combinatorial effects of the configuration of the cationic and the anionic chiral subunits of four zwitterionic chiral stationary phases leading to reversal of elution order of cyclic ˇ3-amino acid enantiomers as ampholytic model compounds, J. Chromatogr. A, 1467 (2016) 178–187

[14] Q. Kharaishvili, G. Jibuti , T. Farkas, B. Chankvetadze, Further proof to the utility of polysaccharide-based chiral selectors in combination with superficially porous silica particles as effective chiral stationary phases for separation of enantiomers in high-performance liquid chromatography, J. Chromatogr. A, 1467 (2016) 163–168

[15] I. Sierra, S. Morante-Zarcero, D. Pérez-Quintanilla, J. Gañán, Novel supports in chiral stationary phase development for liquid chromatography. Preparation, characterization and applications of ordered mesoporous silica particles, J. Chromatogr. A 1363 (2014) 27–40.

[16] G. D'Orazio, M. Asensio-Ramos, C. Fanali, J. Hernández-Borges, S. Fanali, Capillary electrochromatography in food analysis, Trends in Analytical Chemistry 82 (2016) 250–267.

[17] C. Fanali, G. D'Orazio, S. Fanali, Chiral Separations Using Nano-Liquid Chromatography, Scientia Chromatographica 8 (2016) 161-169.

[18] I. Sierra, M. L. Marina, D. Pérez-Quintanilla, S. Morante-Zarcero, M. Silva, Approaches for enantioselective resolution of pharmaceuticals by miniaturised separation techniques with new chiral phases based on nanoparticles and monolithis, Electrophoresis 37 (2016) 2538-2553.

[19] J. S. Beck, J. C. Vartuli, W. J. Roth, M. E. Leonowicz, C. T. Kresge, K. D. Schmitt, C. T. Chu, D. H. Olson, E. W. Sheooard, A new family of mesoporous molecular sieves prepared with liquid crystal templates, J. Am. Chem. Soc., 1992, 114, 10834-10843.

[20] J. Gañán, S. Morante-Zarcero, D. Pérez-Quintanilla, M.L. Marina, I. Sierra, One-pot synthesized functionalized SBA-15 mesoporous silica as a reversed-phase sorbent for solid-phase extraction of endocrine disrupting compounds in milks, J. Chromatogr. A, 1428 (2016) 228–235.

[21] N. Casado, S. Morante-Zarcero, D. Pérez-Quintanilla, I. Sierra, Application of a hybrid ordered mesoporous silica as sorbent for solid-phase multi-residue extraction of veterinary drugs in meat by ultra-high-performance liquid chromatography coupled to ion-trap tandem mass spectrometry, J. Chromatogr. A, 1459 (2016) 24-37.

[22] M. Ide, P. Van Der Voort, The application of ordered mesoporous (organo-)silica' as stationary phase in chromatography, in: M. Aliofkhazraei (Ed.), Comprehensive guide for mesoporous materials, volume 4 : application and commercialization, Nova Science, New York, 2015, pp.231-260.

[23] E. Sánchez-López, A. Salgado, A.L. Crego, M.L. Marina, Investigation on the enantioseparation of duloxetine by capillary electrophoresis, NMR, and mass spectrometry, Electrophoresis 35 (2014) 2842–2847.

[24] E. Sanchez-Lopez, C. Montealegre, M.L. Marina, A.L. Crego, Development of chiral methodologies by capillary electrophoresis with ultraviolet and mass spectrometry detection for duloxetine analysis in pharmaceutical formula- tions, J. Chromatogr. A 1363 (2014) 356–362.

[25] C. A. Weatherly, Y.-C. Na, Y. S. Nanayakkara, R. M. Woods, A. Sharma, J. Lacour, D. W. Armstrong, Enantiomeric separation of functionalized ethano-bridged Tröger bases using macrocyclic cyclofructan and cyclodextrin chiral selectors in high-performance liquid chromatography and capillary electrophoresis with application of principal component analysis, J. Chromatogr. B, 955–956 (2014) 72–80.

[26] S. Wang, C. Han, S. Wang, L. Bai, S. Li, J. Luo, L. Kong, Development of a high speed counter-current chromatography system with Cu(II)-chiral ionic liquid complexes and hydroxypropyl-β-cyclodextrin as dual chiral selectors for enantioseparation of naringenin, J. Chromatogr. A 1471 (2016) 155-163.

[27] X. Yao, T. T. Y Tan, Y. Wang, Thiol–ene click chemistry derived cationic cyclodextrin chiral stationary phase and its enhanced separation performance in liquid chromatography, J. Chromatogr A 1326 (2014) 80-88.

[28] Z.-S. Gong, L.-P. Duan, A.-N. Tang, Amino-functionalized silica nanoparticles for improved enantiomeric separation in capillary electrophoresis using carboxymethyl-β-cyclodextrin (CM-β-CD) as a chiral selector, Microchim Acta 182 (2015) 1297-1304.

[29] S. Orlandini, B. Pasquini, M. Del Bubba, S. Pinzauti, S. Furlanetto, Quality by design in the chiral separation strategy for the determination of enantiomeric impurities: Development of a capillary electrophoresis method based on dual cyclodextrin systems for the analysis of levosulpiride, J. Chromatogr A 1380 (2015) 177-185.

[30] J. Guo, Y. Lin, Y. Xiao, J.Crommen, Z. Jiang, Recent developments in cyclodextrin functionalized monolithic columns for the enantioseparation of chiral drugs, J. Pharm Biomed. Anal 130 (2016) 110–125.

[31] S. Declerck, Y. V. Heyden, D. Mangelings, Enantioseparations of pharmaceuticals with capillary electrochromatography: A review, J. Pharm Biomed. Anal 130 (2016) 81-90.

[32] L-S. Li, Y. Wang, D. J. Young, S-C Ng, T. Y. Tan, Monodispersed submicron porous silica particles functinalized with CD derivatives for chiral CEC, Electrophoresis, 21 (2010) 378-387.

[33] L-F. Zhang, Y-C. Wong, L. Chen, C.B. Ching, S-C. Ng, A facile immobilization approach for perfuncitionalised cyclodextrin onto silica via the Staudinger reaction, Tetrahedron Lett. 40 (1999) 1815-1818.

[34] L. Pasqua, L. Veltri, B. Gabriele, F. Testa, G. Salerno, Progesterone inclusion into cyclodextrin-functionalized mesopoorous silica, J. Porous Mater. 20 (2013) 917-925.

[35] Z-B. Zhang, W-G. Zhang, W-J. Luo, J. Fan, Preparation and enantioseparation characteristics of a novel chiral stationary phase based on mono (6^A-azido-6^A-deoxy)-per(*p*-chlorophenylcarbamoylated)β-cyclodextrin, J. Chromatogr. A 1213 (2008) 162-168.

[36] D. Pérez-Quintanilla, S. Morante-Zarcero, I. Sierra, Preparation and characterization of mesoporous silicas modified with chiral selectors as stationary phase for high-performance liquid chromatography, J. Colloids Int. Sci. 414 (2014) 14–23.

[37] S. Rocchi, A. Rocco, J. J. Pesek, M. T. Matyska, D. Capitani, S. Fanali, Enantiomers separation by nano-liquid chromatography: Use of a novel sub 2µm vancomycin silica hydride stationary phase, J. Chromatogr. A, 1381 (2015) 149-159.

[38] Y. Xiao, S-C. Ng, T.Y. Tang, Y. Wang, Recent development of cyclodextrin chiral stationary phases and their applications in chromatography, J. Chromatogr. A 1269 (2012) 52-68.

[39] R. Huq, L. Mercier, Incorporatiion of cyclodestrin into mesostructured silica, Chem. Mater. 13 (2001) 4512-4519.

[40] J. Zhao, X. Lu, Y. Wang, J. Lv, ´Clik` preparation of a novel ´native-phenylcarbamoylated` bilayer cyclodextrine stationary phase for enhanced chiral differentiation, J. Chromatogr. A 1381 (2015) 253-259.

[41] S.T. Mahmud, L.D. Wilson, Synthesis and characterization of surface-modifed Mesoporous silica materials with β-cyclodextrin, Cogen Chemistry 2 (2016) 1132984.

[42] F. Bressolle, M. Audran, T.-N. Pham, J.J Vallon, Cyclodextrins and enantiomeric separations of drugs by liquid chromatography and capillary electrophoresis: basic principles and new developments, J. Chromatogr. B 687 (1996) 303- 336.

[43] S. C. Ng, T. Ong, P. Fu, C. B. Ching, Enantiomer separation of flavour and fragrance compounds by liquid chromatography using novel urea-covalent bonded methylated β-cyclodextrins on silica, J. Chromatogr. A 968 (2002) 31- 40.

[44] C. R. Mitchell, D. W. Amstrong, in G. Gübitz, M. G. Schmid (Eds), Chiral Separations: Methods and Protocols, Humana Press, Totowa, NJ, 2005 p. 61.

[45] W. L. Jorgensen, J. M. Briggs, J. Gao, A priori calculations of pKa's for organic compounds in water. The pKa of ethane, J. Am. Chem. Soc. 109 (1987) 6857-6858.

Figures

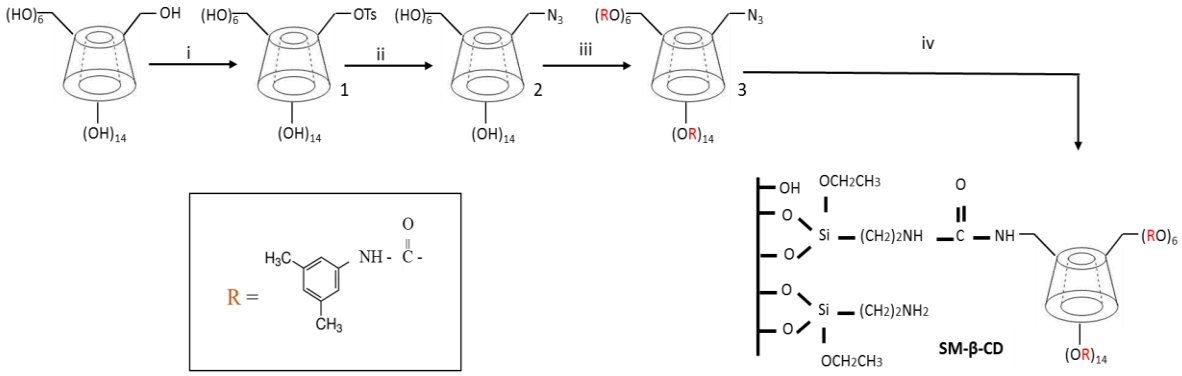

Figure 1 - Preparation of SM-β-CD. (i) Tosyl chloride/pyridine/18h room T[a]; (ii) NaN_3/water/18h 86ºC; (iii) 3,5-dimethyl phenyl isocyanate/pyridine/8h room T[a]; (iv) amino functionalized SM/PPh_3/THF/CO_2.

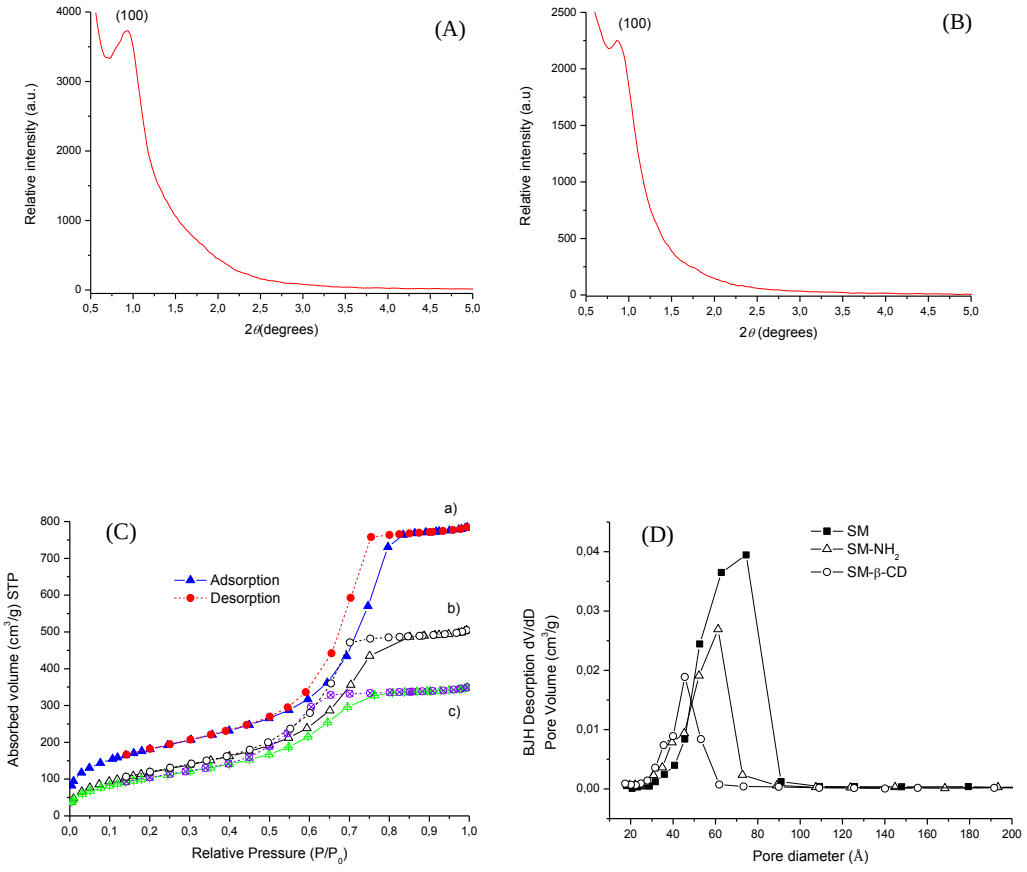

Figure 2 A, B, C and D - (A) XRD pattern of SM. (B) XRD pattern of SM-β-CD. (C) N_2 adsorption-desorption isotherms of a) SM, b) SM-NH_2, c) SM-β-CD. (D) Pore size distribution of the mesoporous silicas.

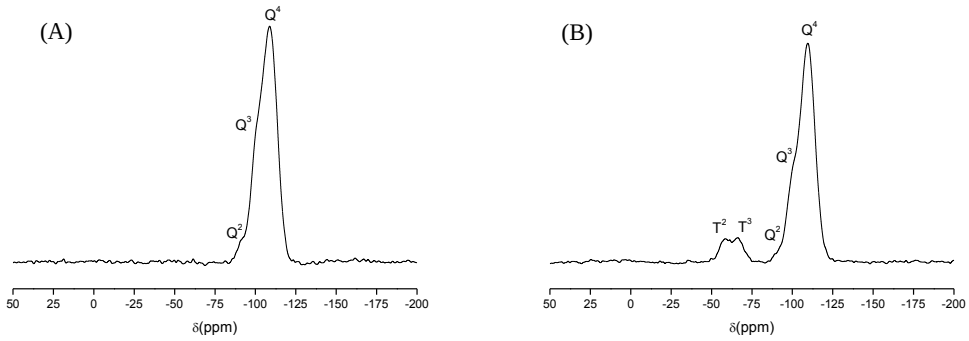

Figure 3 - ^{29}Si MAS NMR of (A) SM and (B) SM-β-CD.

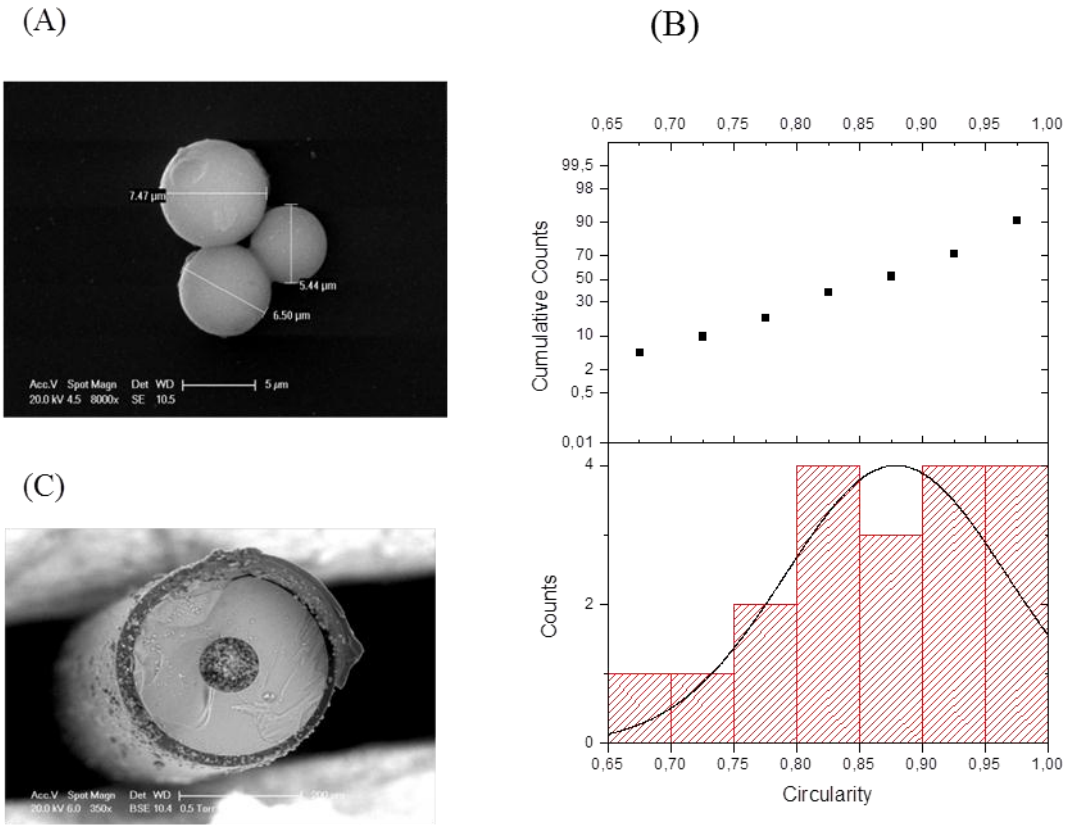

Figure 4 A and B - (A) SEM images of SM. (B) Particle circularity factor of SM. (C) SEM image of cutting section of 100 µm I.D. capillary column packed with SM-β-CD.

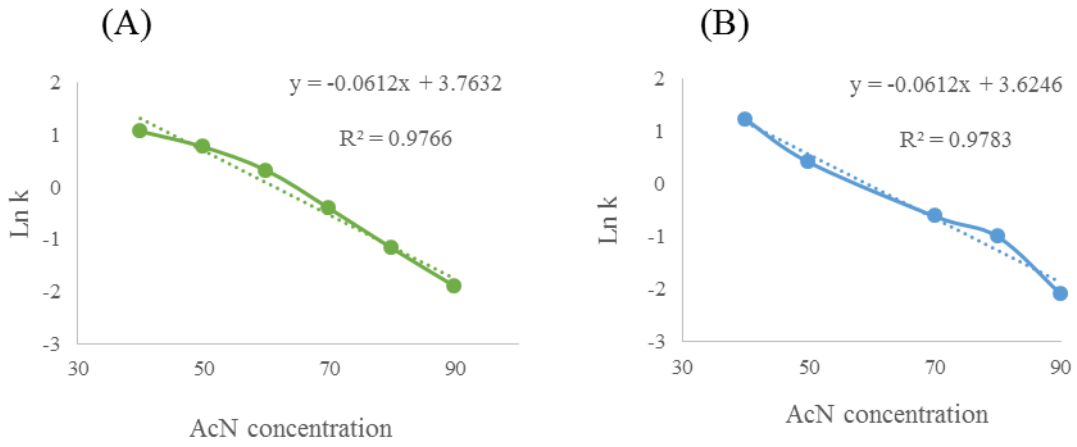

Figure 5 - Linear relation recorded plotting AcN concentration *vs* Ln *k* for (A) 7-methoxyflavanone and (B) flavanone. Analyzed by nano-LC employing a capillary column packed with SM-β-CD under reversed phase conditions (mobile phase AcN/H_2O,10 mM ammonium acetate pH 4.5).

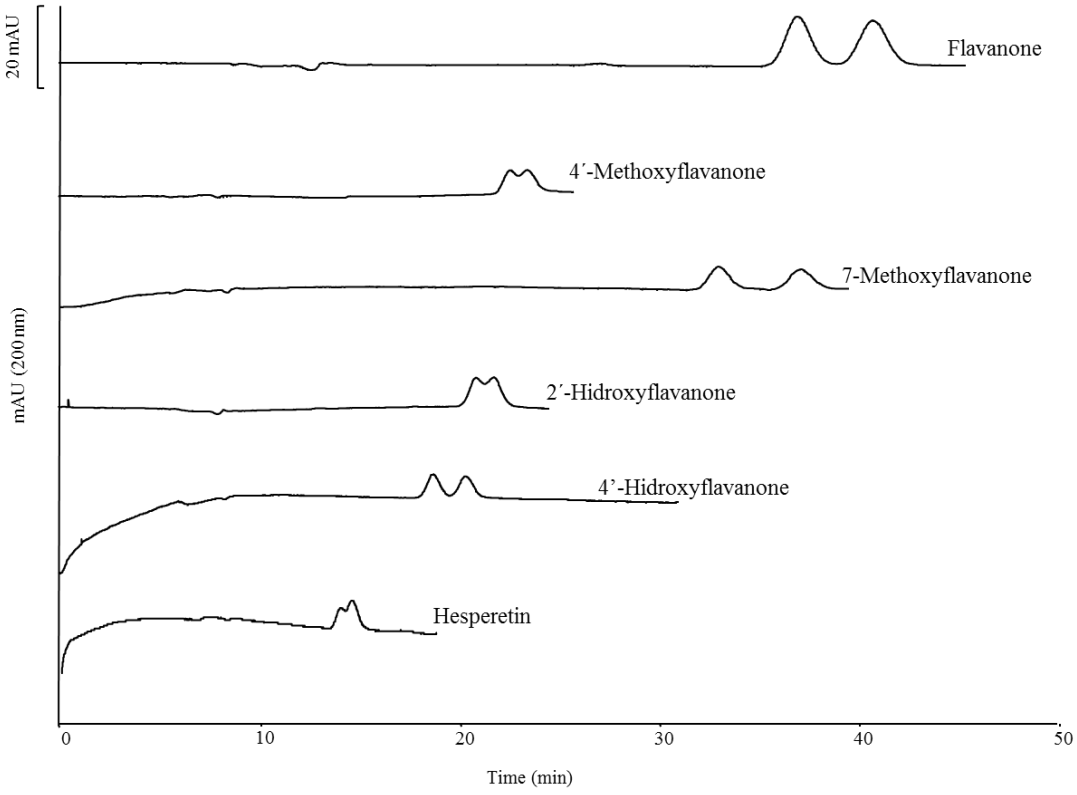

Figure 6 - Enantioseparation of selected flavanones analyzed by nano-LC employing a capillary column packed with SM-β-CD under reversed phase conditions (mobile phase AcN/H_2O,10 mM ammonium acetate pH 4.5 (40/60, v/v)). For other experimental conditions see Table 1.

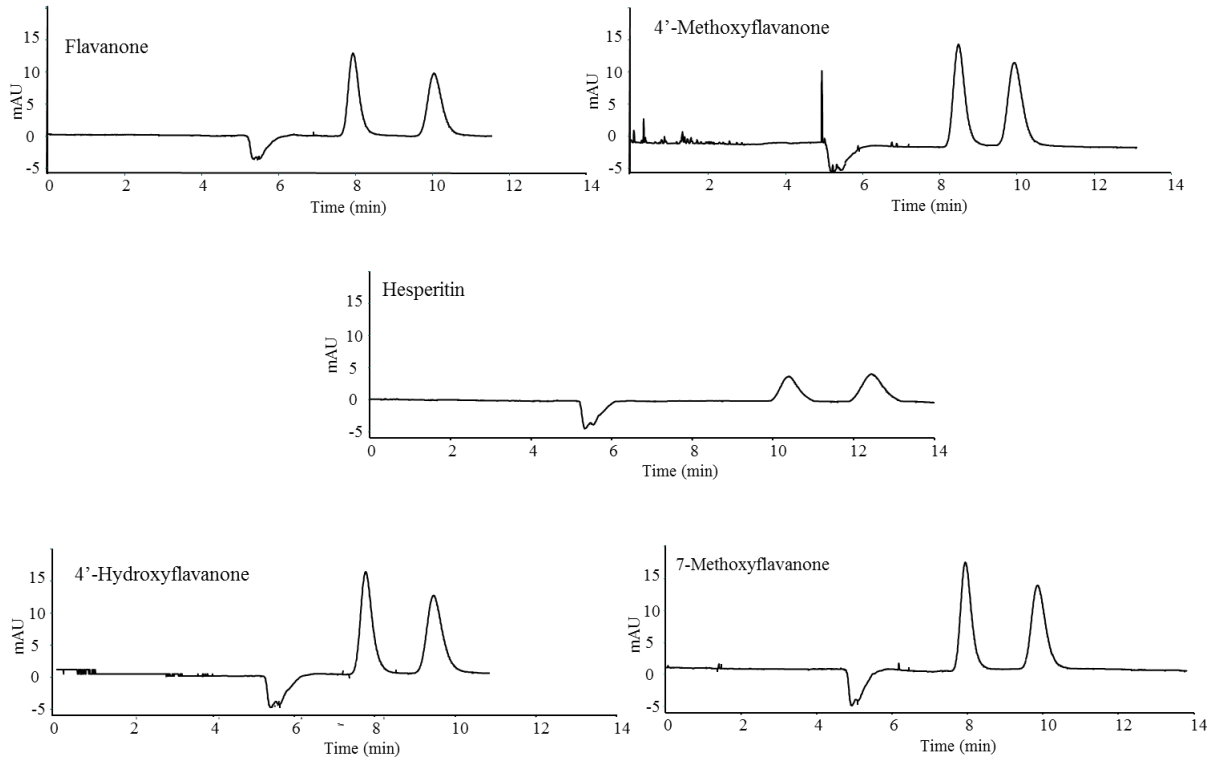

Figure 7 - Enantioseparation of selected flavanones analyzed by nano-LC employing a capillary column packed with SM-β-CD under reversed phase conditions (mobile phase MeOH/H_2O, 10 mM ammonium acetate pH 4.5 (90/10, v/v)). For other experimental conditions see Table 1.

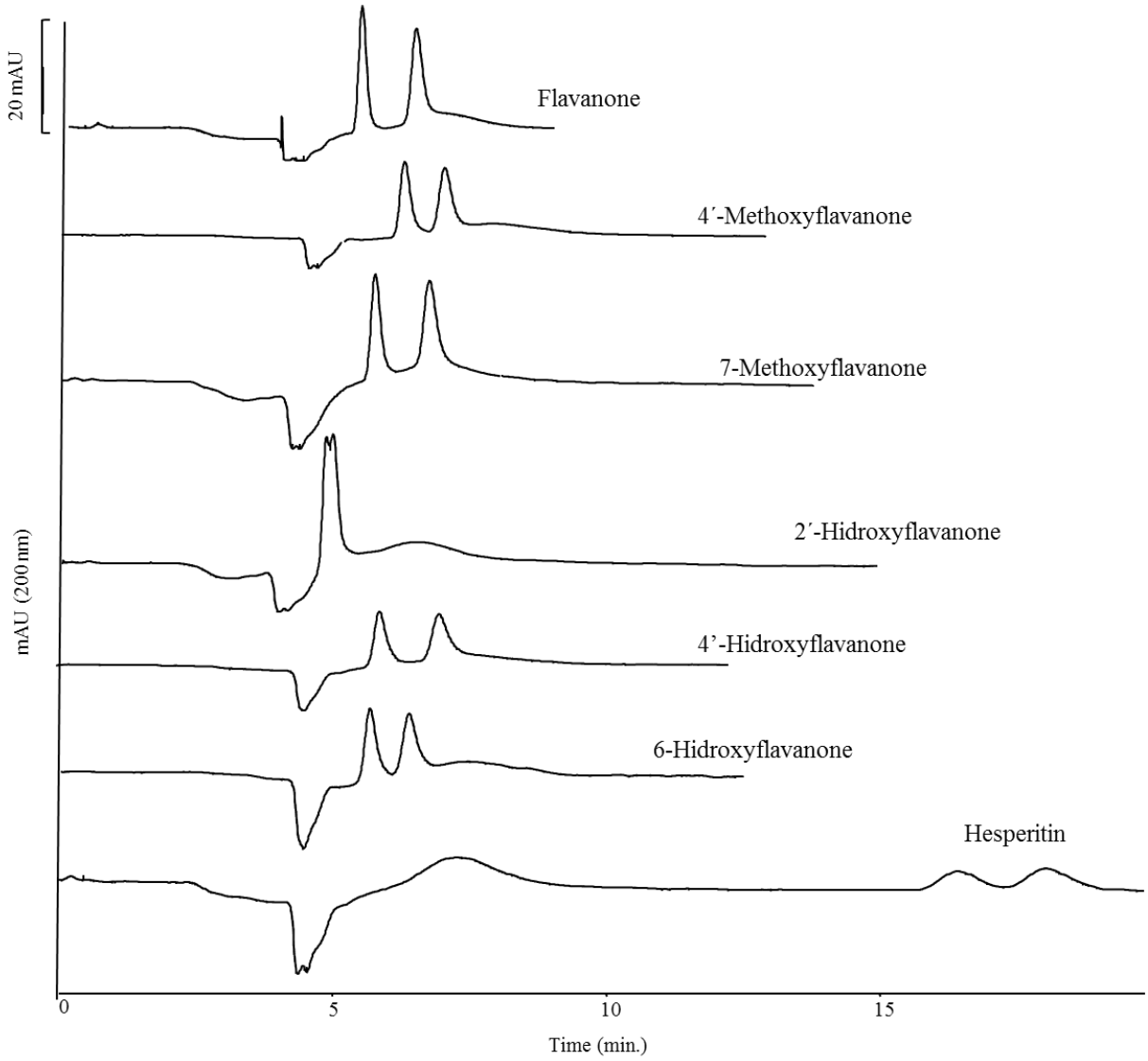

Figure 8 - Enantioseparation of selected flavanones analyzed by nano-LC employing a capillary column packed with SM-β-CD under polar-phase mode (mobile phase 100% MeOH). For other experimental conditions see Table 1.

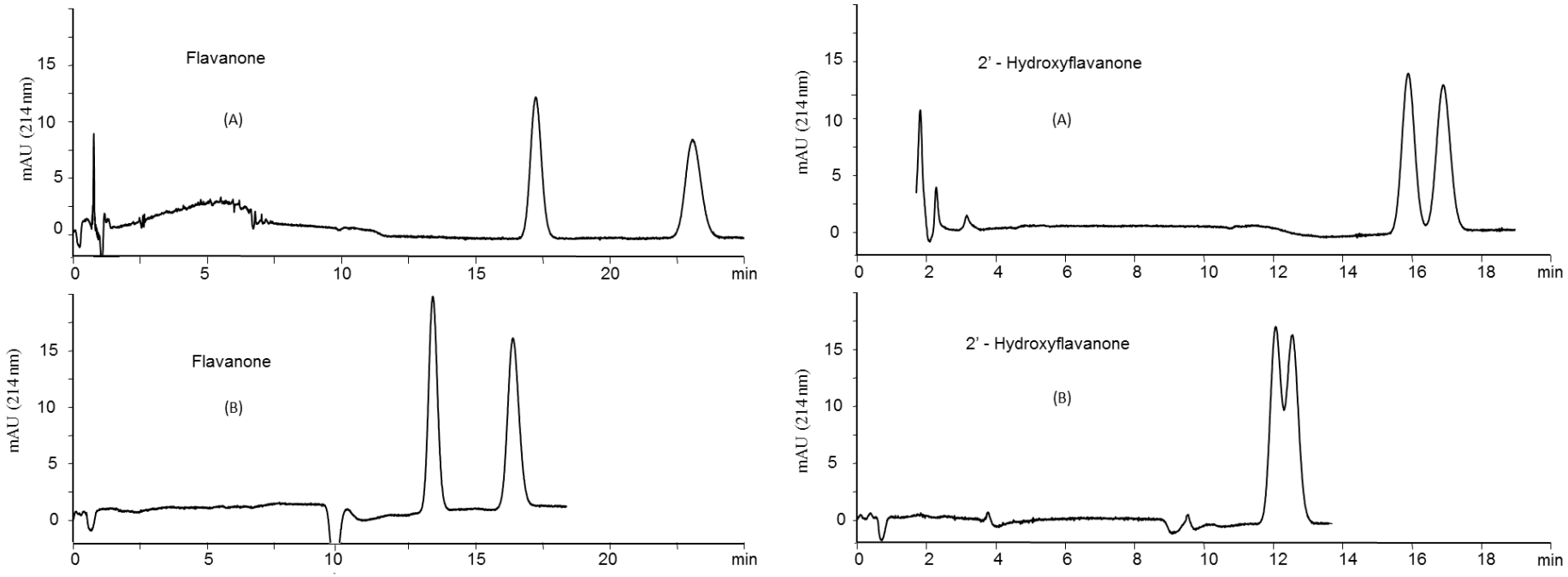

Figure 9 - Enantioseparation of selected flavanones analyzed by CEC employing a capillary column packed with SM-β-CD (A) MeOH/H_2O, 5 mM ammonium acetate pH 6 (90/10, v/v). (B) MeOH/AcN/H_2O, 5 mM ammonium acetate pH 6 (90/5/5, v/v/v). For other experimental conditions see Table 4.

Tables

Table 1

Nano-LC enantiomeric separations of flavanones under reversed-phase condition using a mobile phase based on buffer and acetonitrile.

Compounds	t_{r1}	k_1	t_{r2}	k_2	R_s	α
Flavanone	38.40	3.41	42.30	3.86	1.80	1.10
4´- Methoxyflavanone	22.72	1.83	23.58	1.94	0.60	1.04
7- Methoxyflavanone	33.00	2.93	37.20	3.43	2.00	1.13
2´-Hydroxyflavanone	21.02	1.60	21.89	1.71	0.60	1.04
4´- Hydroxyflavanone	18.00	1.31	19.50	1.50	0.80	1.08
6- Hydroxyflavanone	16.00	0.98	-	-	0	
Hesperetin	13.24	1.11	13.78	1.19	0.50	1.04
Naringenin	15.70	1.57	-	-	0	

Nano-LC experimental conditions:

Capillary column packed with SM-β-CD, 100 μm I.D. x 20 cm packed length; Mobile phase: AcN/H_2O, 10 mM ammonium acetate pH 4.5 (40/60, v/v); flow rate, 281 nL/min; samples concentration, 100 μg/mL.

Table 2

Nano-LC chiral enantiomeric and diastereoisomeric resolutions of flavanones under reversed-phase mode using a mobile phase based on buffer and methanol*.

Compounds	t_{r1}	k_1	t_{r2}	k_2	R_s	α
Flavanone [a]	7.95	0.50	10.04	0.89	3.50	1.26
4´- Methoxyflavanone [a]	8.5	0.63	9.94	0.91	2.30	1.17
7- Methoxyflavanone [a]	8.64	0.61	10.72	1.00	3.1	1.24
2´-Hydroxyflavanone [b]	10.8	0.58	11.64	0.7	1.1	1.08
4´- Hydroxyflavanone [a]	7.52	0.47	9.16	0.80	2.7	1.22
6- Hydroxyflavanone [a]	7.52	0.37	8.60	0.56	1.6	1.14
Hesperetin [a]	10.4	0.96	12.44	1.35	2.2	1.20
Naringenin [c]	38.8	1.98	43.50	2.35	1.6	1.12
Hesperidin [c]	17.6	0.89	20.00	1.15	1.3	1.14
Naringin [c]	17.73	0.91	19.47	1.10	1.00	1.10

* Other experimental conditions as Table 1.

[a] Mobile phase: MeOH/H_2O, 10 mM amonium acetate pH 4.5 (90/10, v/v).

[b] Mobile phase: MeOH/ H_2O, 10 mM amonium acetate pH 4.5 (80/20, v/v).

[c] Mobile phase: MeOH/ H_2O, 10 mM amonium acetate pH 4.5 (70/30, v/v).

Table 3

Nano-LC chiral enantiomeric and diastereoisomeric resolutions of flavanones under polar-phase mode using a mobile phase based on methanol*.

Compounds	t_{r1}	k_1	t_{r2}	k_2	R_s	α
Flavanone	5.43	0.33	6.43	0.57	1.50	1.18
4´- Methoxyflavanone	6.31	0.37	7.05	0.53	1.70	1.12
7- Methoxyflavanone	5.74	0.37	6.73	0.60	1.20	1.17
2´-Hydroxyflavanone	4.92	0.23	5.04	0.26	0.45	1.02
4´- Hydroxyflavanone	5.98	0.33	7.07	0.57	2.00	1.18
6- Hydroxyflavanone	5.72	0.27	6.44	0.43	1.50	1.13
Hesperetin	16.59	2.77	18.23	3.14	1.00	1.10
Naringenin	16.21	2.77			0	
Hesperidin	7.63	0.62			0	
Naringin	6.70	0.52			0	

* Other experimental conditions as Table 1.

Table 4

Chiral separations by CEC.

Compounds	MP: MeOH/H_2O, 5 mM ammonium acetate pH 6 (90/10, v/v)						MP: MeOH/ACN/H_2O, 5 mM ammonium acetate pH 6 (90/5/5, v/v/v)					
	t_{r1}	k_1	t_{r2}	k_2	R_s	α	t_{r1}	k_1	t_{r2}	k_2	R_s	α
Flavanone	17.24	0.66	23.08	1.22	6.24	1.34	13.40	0.41	16.39	0.72	4.29	1.22
4-Methoxyflavanone	19.29	0.86	23.48	1.27	4.14	1.22	15.75	0.71	17.89	0.88	2.63	1.14
7-Methoxyflavanone	19.31	0.86	25.52	1.46	5.67	1.32	15.13	0.60	18.22	0.94	3.75	1.20
2´-Hydroxyflavanone	15.91	0.53	16.90	0.63	1.34	1.06	12.08	0.28	12.57	0.33	0.67	1.04
4-Hydroxyflavanone	17.48	0.69	22.48	1.17	4.80	1.29	12.61	0.34	14.98	0.59	3.12	1.19
6-Hydroxyflavanone	17.40	0.67	19.94	0.92	3.00	1.15	12.60	0.34	14.05	0.50	1.96	1.12

CEC experimental conditions:

Capillary column, 100 µm I.D. packed for 23.0 cm with SM-β-CD, effective and total lengths 23.5 and 33.5 cm, respectively (the packing procedure is the same used for the nano-LC columns) ; MP: mobile phases (see the Table 4), negative polarity, applied voltage, -15 kV; capillary temperature, 25 °C, pressurized column at both ends with 10 bar; injection by pressure: 8 bar x 0.5 min. Samples were diluted in MP at a final concentration of 50 µg/mL.

Hesperetin, naringenin, naringin and hesperidin were also analysed in those conditions without detecting any signal.

A mobile phase of MeOH/H_2O, 5 mM ammonium acetate pH 6 (70/30, v/v) was also tested for the four mentioned compounds but no peaks were detected.

Suplementary material

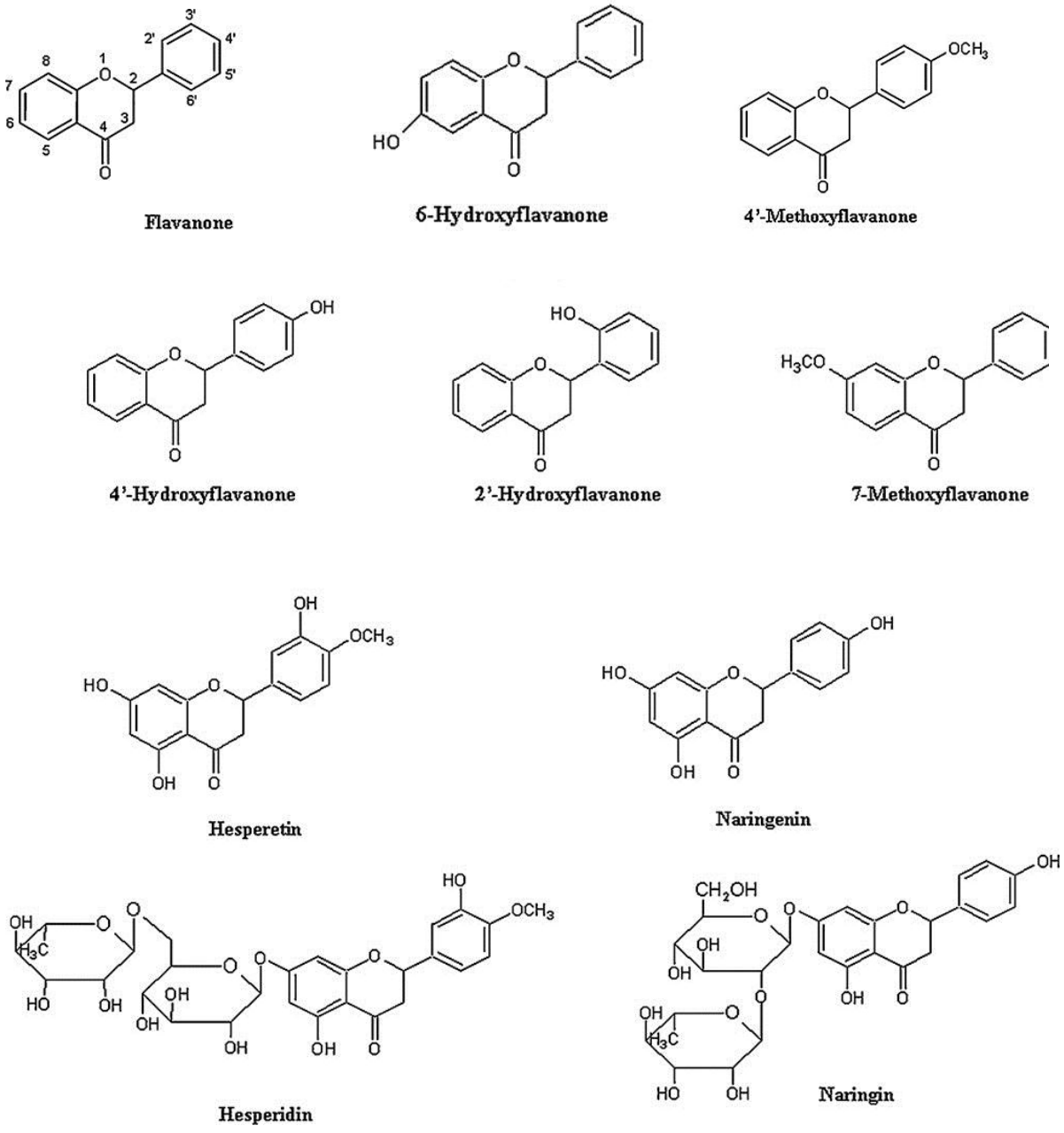

Fig. 1S. Chemical structures of the studied compounds.

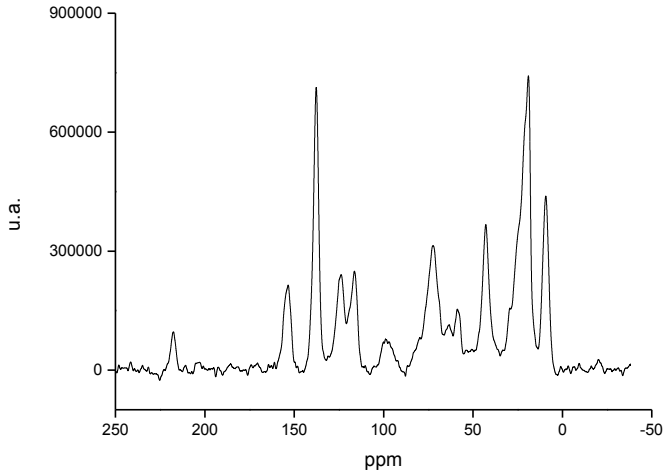

Fig. 2S. ^{13}C MAS NMR of SM-β-CD.

(A) **(B)**

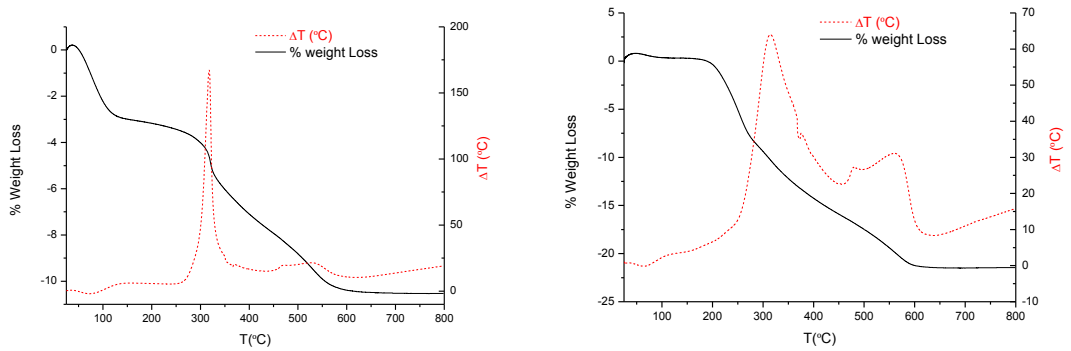

Fig 3S. Thermogravimetric curves and heat flow of (A) SM-NH_2 and (B) SM-β-CD.

Table 1S. Textural properties of the mesoporous silicas.

Material	S_{BET} (m^2/g)	Pore volume (cm^3/g)	Pore diameter (Å)
SM	660.66	1.2	74.5
SM-NH_2	446.60	0.76	61.3
SM-β-CD	389.36	0.54	45.6